Journal of Catalysis 286 (2012) 279–286

Contents lists available at SciVerse ScienceDirect

Journal of Catalysis

journal homepage: www.elsevier.com/locate/jcat

Metallic Pt as active sites for the water–gas shift reaction on alkali-promoted supported catalysts

Jorge H. Pazmiño [a], Mayank Shekhar [a], W. Damion Williams [a], M. Cem Akatay [b], Jeffrey T. Miller [c], W. Nicholas Delgass [a], Fabio H. Ribeiro [a,*]

[a] School of Chemical Engineering, Purdue University, West Lafayette, IN 47907-2100, USA
[b] School of Materials Engineering, Purdue University, West Lafayette, IN 47907, USA
[c] Chemical Technology Division, Argonne National Laboratory, 9700 S. Cass Avenue, Argonne, IL 60439, USA

ARTICLE INFO

Article history:
Received 20 September 2011
Revised 21 November 2011
Accepted 22 November 2011
Available online 24 December 2011

Keywords:
Alkali promotion
Platinum
XANES
Water–gas shift
Na

ABSTRACT

The promotional effect of alkali additives (Na, Li, and K) in the low-temperature (200–250 °C) water–gas shift reaction was studied for Pt/Al_2O_3 and Pt/TiO_2 catalysts. Sodium showed the highest promotion of the turnover frequency (TOF), normalized by Pt on the surface. The TOF at 250 °C and 6.8% CO, 22% H_2O, 37% H_2, and 8.5% CO_2 was enhanced by Na up to 107 times (0.7 s^{-1}) that of Pt/Al_2O_3 (7×10^{-3} s^{-1}) and up to four times (0.7 s^{-1}) the TOF of Pt/P25 TiO_2 (0.2 s^{-1}). The addition of Na on Pt/Al_2O_3 and Pt/TiO_2 changed the reaction orders, with H_2O order increasing by ~0.3, H_2 order increasing by 0.1–0.3, CO_2 order decreasing by 0.2, and CO order decreasing by 0.1–0.2. Together with an approximately 20 kJ $mole^{-1}$ increase in E_a, these data suggest Na creates the same type of active sites on both supports. X-ray absorption spectroscopy (XAS) experiments under WGS conditions indicate that the formation of Pt oxides is dependent on the catalyst preparation method, the type, and the loading of alkali. On catalysts where Pt oxides were observed, no correlation was found between the TOF and the fraction of PtO. The series of $Pt/Na/Al_2O_3$ catalysts with the highest TOF showed fully reduced Pt under WGS conditions. Our results show that the promotion by alkali is caused by the modification of the properties of the support and that the active Pt remains in the metallic state. Thus, for metallic catalysts, alkali is added to the growing list of promoters that modify the support to improve water activation and the WGS reaction rate.

1. Introduction

Noble-metal-based catalysts are attractive materials for the low-temperature water–gas shift (WGS) reaction ($H_2O + CO = H_2 + CO_2$) as they offer greater stability during start-up/shut-down cycles than conventional catalysts. The WGS rates of these catalysts can be enhanced by modifying the support and/or by the addition of promoters. Recent reports have shown substantial improvement in the WGS rate when doping alkali (Na, Li, K) to Pt/CeO_2 [1,2], Pt/TiO_2 [3–5], Pt/ZrO_2 [6,7], and Pt/Al_2O_3 [8]. The nature of such promotion has been explained by the formation of positively charged Pt sites in close contact with the alkali, where the role of the alkali dopant is to assist in providing OH groups proximate to the metal sites [8]. Alternatively, several studies proposed that the enhancement in rate is the result of the increase in the rate of formate decomposition [1,2,6,7] by the weakening of the C—H bonds. This step has been suggested as rate-determining for the low-temperature WGS on Pt/CeO_2 [9] and Pt/ZrO_2 [10], although much controversy still exists about the role of formates as active or spectator species, as summarized in a recent review by Burch et al. [11]. Panagiotopoulou and Kondarides [3] and Zhu et al. [4] have also observed a promotional effect on TiO_2-supported catalysts and concluded that alkali addition creates new sites at the metal/support interface and also increases the reducibility of the support.

Alkali promotion has also been reported for CO oxidation on Pt-based catalysts. Pedrero et al. [12] attributed the promotion effect to the enhancement of the CO disproportionation (or dissociation) reaction, driven by the formation of alkali carbonates. The authors argued that, by leaving unreactive carbon on Pt, the growth of CO monolayers is inhibited and the remaining Pt surface becomes more active. Imbedded in their claim, the higher propensity to leave carbon on the surface is supported by stronger Pt—C bonds as a result of the electron donation from the alkali metal. Experimental [13–15] and theoretical [16] evidence has shown that alkali weakens the C—O bond while strengthening the metal–carbon bond. Other studies, however, have observed the opposite trend (i.e., weakening of Pt—C bond), which may indicate a direct interaction between the alkali metal and CO [17]. Tanaka et al. [18] reported a promotion in the rate for CO oxidation in excess H_2 with

* Corresponding author. Address: School of Chemical Engineering, Purdue University, 480 Stadium Mall Drive, West Lafayette, IN 47907-2100, USA
E-mail address: fabio@purdue.edu (F.H. Ribeiro).

0021-9517/$ - see front matter © 2011 Elsevier Inc. All rights reserved.
doi:10.1016/j.jcat.2011.11.017

the addition of alkali and later proposed that alkali can produce more electron-deficient Pt that weakens the strength of CO adsorption and increases the rate [19]. They showed that such an increase was observed on catalysts with small Pt particles and low alkali loadings (3:1 molar ratio to Pt). Their extended X-ray absorption fine structure (EXAFS) data for catalysts (with and without alkali) after reduction showed the presence of Pt—O bonds on small Pt clusters, but fully reduced Pt was seen as the particle size increased due to either higher calcination temperature or higher alkali loading.

In light of the recent evidence reported by Zhai et al. [8], who claimed that Pt oxides are the active sites for WGS, the current investigation aims to contribute to the understanding of alkali promotion of the WGS on Pt catalysts by combining kinetic analysis with *in situ* X-ray absorption spectroscopy (XAS). Our specific objectives are as follows: (1) to characterize the chemical state of alkali-promoted Pt catalysts under WGS conditions and (2) study the WGS kinetics. We report the rates of water–gas shift on catalysts with alkali (Li, Na, and K) to Pt molar ratios ranging from 7 to 125 and supported on Al_2O_3 and TiO_2.

2. Experimental methods

2.1. Catalyst preparation

All samples used in this study were prepared by the incipient wetness impregnation (IWI) method. Commercial high-surface-area alumina (100 ± 15 m^2 g^{-1}, PV $\sim$ 1.2 ml g^{-1}) AEROXIDE® from Evonik was impregnated with an aqueous solution of $(NH_3)_4Pt(NO_3)_2$ (Aldrich). The amount of support and the concentration of the Pt solution were chosen so as to obtain 0.8 wt.% Pt loading. The samples were dried in vacuum at 60 °C for more than 12 h before a second IWI was done with solutions of the alkali nitrate salts. Prior to preparing the aqueous solutions, the nitrate salts were dried in static air for at least 1 h at 120 °C and cooled to room temperature (RT). The concentrations of the $NaNO_3$ solutions were chosen according to the desired Na:Pt molar ratio, which ranged from 7 to 90. This range would be equivalent to 0.2–1.2 monolayer coverage (assuming 1×10^{19} sites m^{-2}) if the Na was to deposit homogeneously on the alumina support. For convenience, all catalysts were denoted by the corresponding support, alkali:Pt molar ratio, and the type of dopant, i.e., Pt/Al_2O_3–30Na. A second drying cycle in vacuum at 60 °C was conducted for at least 12 h. The catalysts were placed on ceramic boats ($\sim$0.5 g on each) and calcined inside a horizontal tube furnace with flowing air (250 ml min^{-1}) from RT to 250 °C (5 °C min^{-1}) and left at that temperature for 3 h. Next, the samples were purged in He (99.995%) at 250 °C for 10 min and cooled to room temperature in He. About 250 ml min^{-1} of hydrogen (UHP, Praxair) was introduced at room temperature, and the He flow was shut down. For reduction, the temperature was ramped as follows: (1) from RT to 150 °C at 10 °C min^{-1}, stay at 150 °C for 30 min; (2) ramp to 200 °C at 2 °C min^{-1}, stay at 200 °C for 30 min; (3) ramp to 300 °C at 2 °C min^{-1}, stay at 300 °C for 2 h; (4) purge with He (<50 ppm O_2) at 300 °C for 30 min and cool in He to room temperature before exposing to airflow. A second pretreatment, reported in recent literature [8], was also tested for consistency. Three $Pt/Na/Al_2O_3$ catalysts were prepared by calcination in 250 ml min^{-1} flow of air from room temperature to 400 °C (2 °C min^{-1}) and left at that temperature for 4 h and then cooled in air. Finally, the P25 and rutile-supported catalysts were prepared by (incipient) co-impregnation of a solution of 8 wt.% $H_2PtCl_6 \cdot H_2O$ (Aldrich) and $NaNO_3$ (Aldrich) with the appropriate concentrations to obtain 1 wt.% Pt and 4 wt.% Na loadings. The catalyst was then dried and calcined in the same way as for the $Pt/Na/Al_2O_3$ samples, with the difference that the maximum temperature for reduction was set to 250 °C to avoid loss in surface area from strong metal support interactions.

2.2. Characterization

The platinum surface area was measured by H_2 chemisorption in a standard volumetric Micromeritics ASAP 2020 instrument. The basic procedure consisted of evacuation at 300 °C, followed by reduction using Pd-membrane-purified H_2 at 300 °C for 2 h and a second evacuation for 2 h at the same temperature before cooling to the analysis temperature of 35 °C. A Pt/H stoichiometry of 1 was used to estimate Pt surface area. For TiO_2-supported catalysts, the H_2–O_2 titration method [20] was used instead of H_2 chemisorption because the former technique gave closer estimations of the Pt particle size compared to the results obtained by transmission electron microscopy (details included in the supplementary information). After finishing the H_2 chemisorption experiment, the samples were evacuated at 100 °C for 2 h and oxidized in UHP O_2 for 30 min at 100 °C, followed by a second evacuation for 30 min and the analysis at the same temperature. The structure and chemical state of Pt were analyzed by X-ray absorption spectroscopy experiments (XAS) in transmission mode after the following pretreatments: (1) in air at room temperature, (2) *ex situ* reduction in 3.5%H_2/He at 300 °C for 1 h and cooled in that same gas mixture to room temperature, (3) *in situ* reduction in 50 ml min^{-1} of 57%H_2 in Ar at 230 °C, and (4) *in situ* WGS at 230 °C (8%CO, 7%H_2O, 44%H_2, 7%CO_2, balance Ar) with a total flow of 63 ml min^{-1}. The XAS experiments were conducted at the Advanced Photon Source at Argonne National Laboratory. Further details of the experimental setup, experimental references, and the EXAFS data analysis of the Pt L_3 edge are described elsewhere [21]. The coordination numbers obtained by fitting the EXAFS were used to estimate particle sizes following the calibration developed by Miller et al. [22]. Based on previous findings [23], the adsorption of CO on Pt was examined by subtracting the near edge spectrum of each catalyst under reducing conditions from the spectrum of that catalyst taken under WGS conditions at the same temperature to produce the ΔXANES spectrum.

2.3. Catalytic tests and kinetic measurements

The same reactor setup described in Bollmann et al. [24] was used for kinetic analysis. It consists of four parallel reactors operating in differential plug flow mode. The effluent of the reactors can be periodically injected into two Agilent 6890 gas chromatographs, each equipped with a Carboxen 1000 packed column and a thermal conductivity detector (TCD). A series of automatic switching valves facilitates the analysis of the feed gas prior to each injection of the gases coming from the reactors. All samples were pelletized, ground, and sieved to obtain grain size between 0.12 and 0.25 mm. Depending on the sample, 0.2–0.4 g of the alkali-promoted catalysts and about 1 g of Pt/Al_2O_3 were used to conduct the analysis in the range of 200–250 °C while keeping the total CO conversion below 10%. Catalysts were first heated in 50 ml min^{-1} Ar gas to 100 °C and then reduced in a 25% H_2, 75% Ar mixture ramping from 100 °C to 300 °C at 5 °C min^{-1} and left reducing for 2 h. Next, the samples were exposed to our standard WGS conditions (6.8% CO, 8.5% CO_2, 21.9% H_2O, 37.4% H_2, balance Ar) at 300 °C with a total flow rate of 75.4 standard ml min^{-1} for about 4 h. The temperature was then decreased accordingly to obtain CO conversions below 10%, and the conversion was monitored with time until it reached steady conditions (below 5% variation in the measured value). After this $\sim$20 h WGS pretreatment, the reactors were cooled to 230 °C to measure orders of reaction.

Once steady-state conditions were reached, the WGS kinetics were determined. The estimation of apparent activation energy was obtained by varying the temperature over a range of 40–50 °C, while keeping the gas concentrations at standard conditions. Reaction orders were measured at 230 °C for all

alkali-promoted Pt/Al_2O_3 samples by changing the gas concentrations in the ranges of 4–21% CO, 5–25% CO_2, 11–34% H_2O, and 14–55% H_2. During all experiments, the carbon mass balance was higher than 95% and no methanation was observed. Mass and heat transfer limitations were absent according to the experimental observations described in supplementary information. The rate at our standard gas composition was checked periodically to account for deactivation. Upon completing the analysis, the reactors were cooled to room temperature under Ar flow and passivated in 2% O_2/Ar mixture for 2 h before exposing the catalysts to ambient conditions.

3. Results

3.1. Alkali promotion and water–gas shift kinetics

In agreement with previous reports [2–5,8,25], we observed that the addition of alkali increased the WGS rate per mole of Pt (250 °C) by as much as a factor of 70 compared to Pt/Al_2O_3. The data on $Pt/Na/Al_2O_3$ catalysts are described first since the addition of Na resulted in the highest enhancement of the water–gas shift rate as compared to Li or K at the same alkali:Pt ratio (Table 1). To put our results in perspective, the optimum rate of our $Pt/Na/Al_2O_3$ catalysts is compared with that reported by Zhai et al. [8] in Table 2 and other non-promoted WGS catalysts, as shown in Table S1. A volcano-like curve for the WGS rate was observed with the addition of Na, as seen in Fig. 1. Here, most of the data correspond to catalysts prepared by calcination up to 250 °C followed by reduction at 300 °C (refer to Section 2.1), but the data for three $Pt/Na/Al_2O_3$ catalysts prepared by calcination up to 400 °C are also included. Under our experimental conditions, the WGS rate per total mole Pt was maximized with a nominal Na:Pt ratio around 30 (28 by ICP). The apparent activation energy for $Pt/Na/Al_2O_3$ samples (Na:Pt ratio > 7), measured around 230 °C, was higher at 80–90 kJ $mole^{-1}$, compared to that of the non-promoted catalyst at 65 kJ $mole^{-1}$.

Changes in WGS reaction orders were evidenced with the addition of Na to Pt/Al_2O_3. Table 1 shows that for all Na:Pt molar ratios the water order increased from 0.72 for the non-promoted sample to 0.85–1 for the promoted samples, while the CO_2 order decreased from 0.2 to −0.2. With the exception of Pt/Al_2O_3–7Na, the apparent activation energy, E_a, showed values between 78 and 89 kJ $mole^{-1}$, which are 13–24 kJ $mole^{-1}$ higher than those seen for Pt/Al_2O_3–0Na. That change was accompanied by a decrease (from 0.09 to ∼−0.05, on average) in the CO order and an increase from −0.4 to −0.3 to −0.2 in the H_2 order for the promoted samples. A similar trend in the water and CO_2 reaction orders was observed on Li- and K-promoted Pt/Al_2O_3 samples. The most notable differences were

Table 1
Water–gas shift kinetic data for 0.82 wt.% Pt/Al_2O_3 and alkali-doped (Li, Na, K) catalysts. Orders of reaction were measured at 230 °C for all $Pt/Na/Al_2O_3$ and $Pt/Li/Al_2O_3$, and 250 °C for $Pt/K/Al_2O_3$ samples. Rates and TOF are reported at 250 °C, 6.8% CO, 8.5% CO_2, 21.9% H_2O, 37.4% H_2, and 1 atm.

Catalyst	Rate/10^{-2} mole H_2 mole Pt^{-1} s^{-1}	Pt disp. */%	TOF [e]/s^{-1}	E_a/kJ $mole^{-1}$	H_2O(±0.07)	CO_2(±0.05)	CO(±0.05)	H_2(±0.05)
Pt/Al_2O_3 [a]	0.6	70	0.9×10^{-2}	74 ± 2	0.7	0.0	0.1	−0.4
Pt/Al_2O_3–0Na [b]	0.2	35	0.7×10^{-2}	65 ± 2	0.7	0.2	0.1	−0.3
Pt/Al_2O_3–7Na [b]	0.7	21	0.03	65 ± 2	1.0	−0.1	0.1	−0.3
Pt/Al_2O_3–12Na [b]	2.5	23	0.11	78 ± 1	1.0	−0.2	−0.1	-0.3
Pt/Al_2O_3–20Na [b]	11	26	0.43	85 ± 1	1.1	−0.3	−0.1	−0.3
Pt/Al_2O_3–20Na [c]	7	14	0.49	85 ± 2	1.0	−0.2	−0.1	−0.2
Pt/Al_2O_3–30Na [b,f]	16	22	0.71	76 ± 5	1.0	−0.2	0.0	−0.2
Pt/Al_2O_3–30Na [b,d]	13	21	0.59	87 ± 2	0.9	−0.2	0.0	−0.2
Pt/Al_2O_3–40Na [b]	12	26	0.46	88 ± 1	1.0	-0.2	0.0	−0.2
Pt/Al_2O_3–50Na [b]	11	19	0.55	86 ± 2	1.0	−0.2	−0.1	−0.2
Pt/Al_2O_3–60Na [b]	6	15	0.41	89 ± 2	1.0	−0.3	−0.1	−0.2
Pt/Al_2O_3–90Na [c]	4	5	0.88					
Pt/Al_2O_3–12Li [c]	1.4	21	0.06	70 ± 2	0.7	−0.1	0.2	−0.3
Pt/Al_2O_3–50Li [c]	5.2	25	0.20	89 ± 1	0.7	−0.1	−0.1	−0.3
Pt/Al_2O_3–90Li [c]	4.4	16	0.26	92 ± 2	0.8	−0.1	0.0	−0.3
Pt/Al_2O_3–90Li [b]	4.0	23	0.18	88 ± 2	0.8	−0.1	−0.1	−0.2
Pt/Al_2O_3–125Li [c]	3.2	16	0.20	97 ± 3	0.8	−0.2	−0.1	−0.3
Pt/Al_2O_3–12 K [c]	0.9	10	0.08	73 ± 1	1.1	−0.2	0.0	−0.2
Pt/Al_2O_3–50 K [c]	2.8	11	0.26	75 ± 3	1.0	−0.2	0.1	−0.3
Pt/Al_2O_3–90 K [c]	1.2	6	0.20	73 ± 2	1.0	−0.2	0.2	−0.3

[a] Catalyst (2.6 wt.% Pt) prepared with a different Al_2O_3 (Puralox KR-160 from Sasol).
[b] Prepared by calcination at 250 °C, reduction up to 300 °C.
[c] Prepared by calcination at 400 °C.
[d] Repeat.
[e] Normalized by H_2 chemisorption*. TOF = (mole H_2 g^{-1} s^{-1})/(mole Pt surface g^{-1}).
[f] ICP results showed 0.65 wt.% Pt and 2.17 wt.% Na. Na/Pt molar ratio of 28.

Table 2
Comparison of water–gas shift rates at 250 °C on Na-promoted Pt/Al_2O_3 catalysts.

Catalyst	Na:Pt [a]	Rate/μmole H_2 g_{cat}^{-1} s^{-1}	Rate/10^{-2} mole H_2 mole Pt^{-1} s^{-1}	E_a/kJ $mole^{-1}$	Reference
0.82% Pt/Al_2O_3	0	0.1[b]	0.3[b]	65 ± 2	This work
0.82% Pt/2.97% Na/Al_2O_3	30	9[b]	21[b]	76 ± 5	This work
2.3% Pt/Al_2O_3	0	4	3	65	Zhai et al. [8]
2.3% Pt/2.75% Na/Al_2O_3	10	40	34	50	Zhai et al. [8]

[a] Molar ratio.
[b] WGS rate corrected to Zhai et al. [8] conditions (11% CO, 26% H_2O, 26% H_2, 7% CO_2, 1 atm).

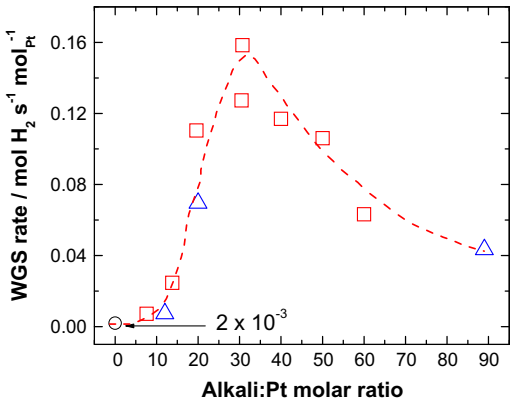

Fig. 1. Water–gas shift rates at 250 °C on 0.82 wt.% Pt/Na/Al_2O_3 catalysts under standard gas compositions of 6.8% CO, 8.5% CO_2, 21.9% H_2O, 37.4% H_2, balance Ar. Data in squares (□) correspond to catalysts prepared by calcination at 250 °C and reduction at 300 °C, while data in triangles (△) correspond to catalysts prepared by calcination up to 400 °C.

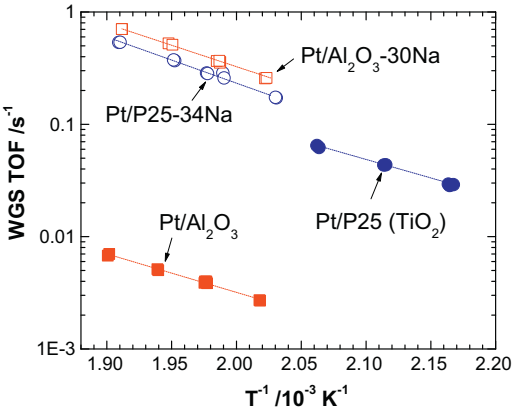

Fig. 2. Arrhenius plot for 0.82 wt.% Pt/Al_2O_3 (■) and 1 wt.% Pt/P25 (●) and their corresponding Na-promoted catalysts Pt/Al_2O_3–30Na (□) and Pt/P25–34Na (○) under standard WGS gas composition of 6.8% CO, 8.5% CO_2, 21.9% H_2O, 37.4% H_2, balance Ar.

the progressive increase in water order with the addition of Li and the positive CO order observed on all Pt/K/Al_2O_3 catalysts. The activation energy on the Li-doped samples also increased from 70 kJ mole^{-1} up to 97 kJ mole^{-1} with the highest Li:Pt ratio. No similar trend was seen on Pt/K/Al_2O_3 samples which showed a constant E_a around 74 kJ mole^{-1}.

When normalizing the rate by Pt surface area measured by H_2 chemisorption, the turnover frequency (TOF, 250 °C) of the Pt/Na/Al_2O_3 catalysts prepared by calcination at 250 °C and reduction at 300 °C increased with the addition of Na, reaching an optimal value of 0.7 s^{-1}. With higher Na loadings, the TOF values were lower but within a factor of 2 of the optimal TOF. Note that Pt/Al_2O_3–90Na catalyst, which was prepared by calcination at 400 °C, exhibited the highest TOF of 0.9 s^{-1}. This value, however, is the result of normalizing the rate by a (3–4 times) lower Pt dispersion as the values measured on the rest of the catalysts in the series. For the other alkali-promoted catalysts, a maximum TOF of 0.26 s^{-1} was achieved with a Li:Pt molar ratio nearing 90, whereas the same TOF of 0.26 s^{-1} was obtained with a K:Pt ratio of 50.

Table 3 shows the corresponding results for catalysts on titania supports. The addition of Na to Pt/rutile and Pt/P25 resulted in similar changes in all the reaction orders and activation energies as observed for the Na-doped Pt/Al_2O_3 catalysts. The Arrhenius plot in Fig. 2 compares the alkali-promoted rate per mole of surface Pt (TOF) of Pt/Al_2O_3 and Pt/P25 with similar Na:Pt molar ratios. The rates on both catalysts were within a factor of 2 across the temperature range we studied (210–250 °C). The promotion of the rate, however, was found to vary depending on the structure of the TiO_2 support. While Pt/rutile–34Na increased the turnover frequency at 250 °C by a factor of two relative to the unpromoted catalyst, the corresponding Pt/P25–34Na showed a factor of four enhancement of the TOF. The promotion effect becomes more evident at higher temperatures due to the increase in E_a. The TOF at 300 °C increased by three times on Pt/rutile and seven times on Pt/P25 with the addition of sodium in a molar ratio to Pt of 34 (4 wt.% Na). To better compare our results, the WGS TOFs were corrected to the gas compositions used by Zhu et al. [4] and those used by Koryabkina et al. [26] when testing a CuO/Al_2O_3 catalyst (Table S2). The TOF at 300 °C on our Pt/Na/P25 catalyst was nine times more than the TOF of 0.42 s^{-1} on CuO/Al_2O_3 and compares within a factor of 2.7 with findings from Zhu et al. [4].

3.2. In situ X-ray absorption spectroscopy (XAS)

The chemical state of Pt under WGS conditions was studied by X-ray absorption spectroscopy (XAS) in order to test the previous hypothesis [8] regarding partially oxidized Pt being the active site on Pt/alkali/Al_2O_3 catalysts. The Pt L_3 XANES in Fig. 3 for the Pt/Na/Al_2O_3 catalysts that were pretreated by calcination in air at 250 °C, reduction in H_2 at 300 °C followed by He passivation and exposure to air at room temperature showed the presence of oxidized Pt when the data were collected at ambient conditions. Here, a monotonic increase in the white line intensity is observed with the addition of Na up to a Na:Pt molar ratio of 40. However, the XANES of the Pt/Al_2O_3–60Na did not fall in that trend as it showed a lower intensity white line, characteristic of metallic platinum. As shown by the XANES for Pt/Al_2O_3–30Na in Fig. 4, platinum was completely reduced (see comparison with Pt/Al_2O_3 in Fig. S1) upon *in situ* reduction in 57% H_2/Ar at 230 °C and remained reduced upon exposure to the WGS gas mixture. Note that a shift of the Pt L_3 white

Table 3
Water–gas shift kinetic data for 1 wt.% Pt/Na/rutile and 1 wt.% Pt/Na/P25 catalysts. Orders of reaction for all samples (except Pt/P25–0Na) were measured at 230 °C.

Catalyst	Rate /10^{-2} mole H_2 mole Pt^{-1} s^{-1}		Pt disp./%	Pt disp. by TEM/%	TOF [a]/s^{-1}		E_a/kJ mole^{-1}	H_2O (±0.05)	CO_2(±0.03)	CO(±0.03)	H_2(±0.03)
	250 °C	300 °C			250 °C	300 °C					
Pt/rutile–0Na	6	19	48	54	0.13	0.40	56 ± 1	0.68	0.0	0.3	−0.7
Pt/rutile–13Na	8	38	37		0.21	1.04	80 ± 1	0.98	−0.1	0.0	−0.3
Pt/rutile–34Na	6	28	23	41	0.28	1.27	76 ± 1	0.82	−0.2	0.1	−0.3
Pt/P25–0Na [b]	8	25	40	54	0.19	0.62	60 ± 2	0.63	0.0	0.2	−0.6
Pt/P25–34Na	15	70	28	44	0.72	3.74	77 ± 3	0.86	−0.2	0.1	−0.4

[a] Normalized by Pt surface area measured by H_2–O_2 titration. TOF = (mole H_2 g^{-1} s^{-1})/(mole Pt surface g^{-1}).
[b] Orders of reaction measured at 190 °C.

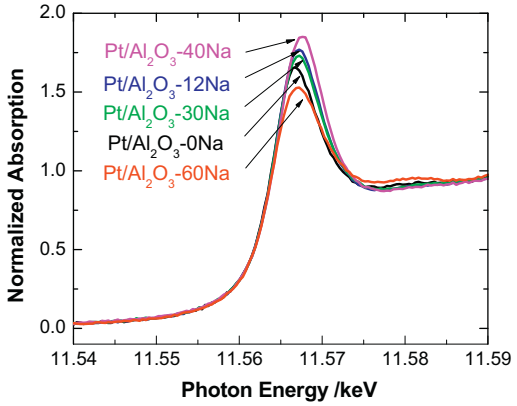

Fig. 3. Pt L_3 XANES spectra from 11.54 to 11.59 keV for 0.82 wt.% Pt/Na/Al_2O_3 in air at RT before WGS reaction. Catalysts were prepared by calcination at 250 °C, reduction at 300 °C, passivation, and exposure to air at RT.

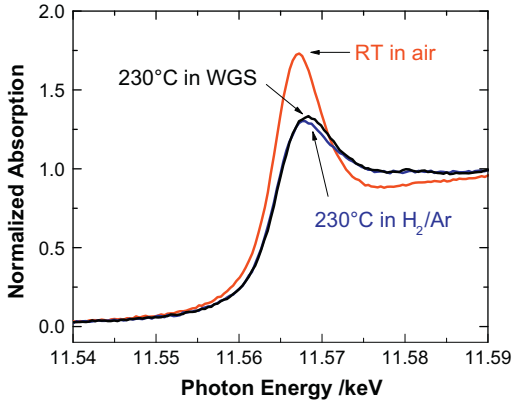

Fig. 4. Pt L_3 XANES spectra from 11.54 to 11.59 keV for 0.82 wt.% Pt/Na/Al_2O_3 (Pt/Al_2O_3–30Na). Catalyst was prepared by calcination at 250 °C, reduction at 300 °C, passivation, and exposure to air at RT.

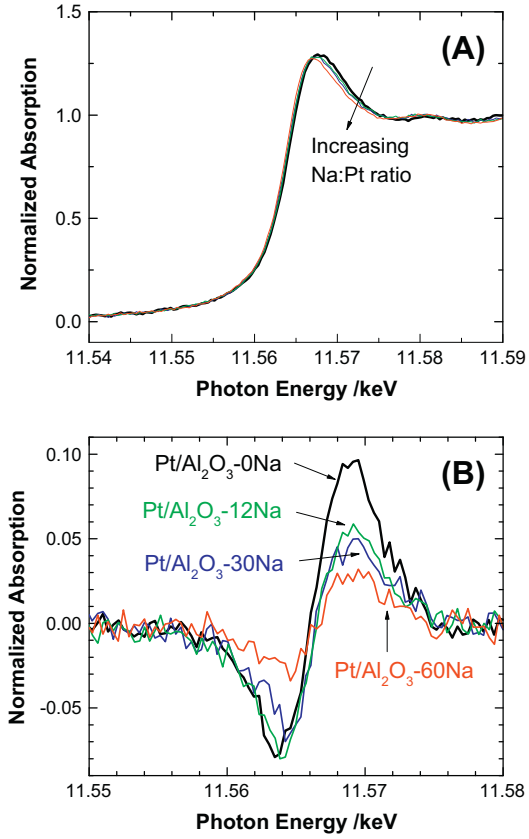

Fig. 5. Pt L_3 XANES (A) and ΔXANES (B) spectra from 11.54 to 11.59 keV for 0.82 wt.% Pt/Na/Al_2O_3 under WGS conditions (8% CO, 7% H_2O, 44% H_2, 7% CO_2, balance Ar) at 230 °C. Catalysts were prepared by calcination at 250 °C, reduction at 300 °C, passivation, and exposure to air at RT.

line was observed under WGS conditions, which is typical of CO adsorbed on Pt [23,27]. The EXAFS fittings in Table S3 confirmed that Pt was completely reduced either by *ex situ* H_2/He treatment (refer to Section 2.2) or by flowing H_2/Ar *in situ* and that Pt stayed metallic under WGS conditions, irrespective of the amount of Na. A comparison of the XANES for all the Pt/Na/Al_2O_3 catalysts, collected during WGS, is presented in Fig. 5 along with the ΔXANES obtained by subtracting the XANES of the reduced catalyst from that under WGS. The particle size on fresh catalysts was estimated by EXAFS to be between 1.5 and 2.0 nm for Pt/Al_2O_3 and Pt/Na/Al_2O_3 up to a Na:Pt molar ratio of 40. However, higher Na content led to an increase in particle size to about 4.0 nm for Pt/Al_2O_3–60Na. Lastly, Table S3 reveals that used samples (after WGS kinetic measurements) exhibited larger particle size at all Na loadings.

While the Pt/K/Al_2O_3 catalysts also showed complete reduction of Pt under WGS conditions, a different behavior was observed on the Pt/Li/Al_2O_3 samples. The results from the EXAFS fittings in Table S4 confirmed the presence of Pt—O bonds at 2.03 Å on Pt/Al_2O_3–90Li and Pt/Al_2O_3–125Li. Interestingly, the XANES for the catalyst with lower Li loading, i.e., Pt/Al_2O_3–13Li, showed fully reduced Pt, with an average particle size of 3.0 nm. On the other hand, Pt/Al_2O_3–90Li and Pt/Al_2O_3–125Li showed about 40% PtO and particle sizes of 6.0 and 9.0 nm, respectively (Table S4, Fig. S2). In principle, one can calculate the fraction of metal and oxide from XANES and also (independently) from EXAFS. In the absence of proper XANES references to determine the fraction of each phase, we used the fitted coordination number (CN) for Pt–O (N_{Pt-O}) obtained from EXAFS analysis. The main idea behind this approach is that EXAFS probes all Pt in the sample, and in mixtures, the fitted coordination number (CN) corresponds to the real CN multiplied by the fraction of that phase. Thus, the fitted CN is always lower than that for pure phases (i.e., Pt or PtO). From the edge position, we identified the oxidized platinum phase as Pt^{2+}, which has square planar geometry with a Pt coordination number (N_{Pt2+}) of 4. Furthermore, in our experience with Pt^{2+}, we have never seen the true CN deviate from ~4, regardless of its state of dispersion. Thus, we assume that $N_{Pt2+} = 4$. Then, for example, if the fitted coordination number was 2, then the fraction as an oxide in the 2+ state (f_{PtO}) would be $f_{PtO} = N_{Pt-O}/N_{Pt2+}$ or 0.5 (2/4). To obtain the coordination number of the metallic phase of Pt (N^*_{Pt-Pt}), we divide the fitted N_{Pt-Pt} by the fraction of metallic Pt, $(1 - f_{PtO})$. From (N^*_{Pt-Pt}), one can estimate the particle size of the cluster by using the correlation between CN and size reported in [22], and the dispersion using the relation: size (nm) = 1.1/Pt dispersion. The results of these calculations are given in Table S5 and show that the fraction of Pt^0 decreases with Li loading. It is interesting to note that although Pt/Al_2O_3–90Li and Pt/Al_2O_3–125Li showed oxidized Pt, the perturbation in the Pt L_3-edge under WGS conditions was similar to that of fully reduced Pt (Fig. S3). The shape of the ΔXANES, shown in Fig. S4 for Pt/Al_2O_3–90Li, is identical to that of Pt/Al_2O_3, but shifted to higher energy due to the contribution of oxidized Pt.

Additional XAS measurements were taken to investigate the effect of different pretreatments on the oxidation of Pt. The data for two of the Pt/Na/Al_2O_3 catalysts prepared by calcination in air at 400 °C (no reduction) are summarized in Table S4. Unlike the case of Pt/Na/Al_2O_3 catalysts prepared by calcination at 250 °C and reduction at 300 °C, the results on these two samples showed

Pt–O bonds at 2.04 Å after the same *ex situ* reduction (Section 2.2) was conducted in 3.5% H_2/He at 300 °C for 1 h, followed by cooling in He (no exposure to air). On Pt/Al_2O_3–20Na, about 15% of the platinum was in the form of PtO. As the Na:Pt molar ratio was increased to 90, 40% of the Pt was oxidized. Both catalysts showed large Pt particles as compared to the set of $Pt/Na/Al_2O_3$ catalysts prepared by calcinations at 250 °C and reduction at 300 °C. Based on the same procedure described for $Pt/Li/Al_2O_3$, the fraction of surface (metallic) Pt was estimated (Table S5). Consistent with the trend on $Pt/Li/Al_2O_3$, this fraction decreased with the Na:Pt molar ratio such that Pt/Al_2O_3–20Na had 1.6 times more surface Pt^0 than Pt/Al_2O_3–90Na. We note that in no case was Pt^{4+} detected.

4. Discussion

4.1. Interpretation of kinetic results

The comparison (in Table 2) of the WGS rate of our optimum $Pt/Na/Al_2O_3$ formulation with that reported by Zhai et al. [8] confirms the existence of the alkali-promotional effect. Note that the promotion we obtained differs from that of Zhai et al.[8] because their WGS rate for Pt/Al_2O_3 was ~10 times higher than the rate we have measured on a series of different Pt/Al_2O_3 catalysts (Table 1), including the one used for this study (Pt/Al_2O_3–0Na). Also note that, contrary to our observations, the activation energy extracted from Zhai et al. [8] data showed a 15 kJ mole^{-1} decrease on the Na-promoted catalyst with respect to their Pt/Al_2O_3, which had an activation energy of 65 kJ mole^{-1}. Despite these differences, our WGS rates per mole Pt per second at 250 °C, when corrected to the inlet gas concentrations of Zhai et al. [8] using our measured orders of reaction, compare within a factor of 1.6 to the values (extrapolated to 250 °C) extracted from Fig. 3 in [8]. An increase by up to a factor of 70 was obtained in our case, based on the rate per mole Pt we measured on alkali-free Pt/Al_2O_3. Although Pt/Al_2O_3–90Na exhibits the highest TOF of 0.9 s^{-1}, the drop in Pt surface area suggests that the alkali interacted differently with Pt as it did on samples with lower Na content. To maintain consistency, we compared rates among the catalysts with similar Pt dispersions and found that Pt/Al_2O_3–30Na has the optimal TOF (250 °C) of 0.7 s^{-1}. When correcting for the gas composition reported in Panagiotopoulou and Kondarides [28] (3% CO, 6% CO_2, 10% H_2O and 20% H_2), our turnover frequency at 250 °C (3.7×10^{-3} s^{-1}) for Pt/Al_2O_3–0Na is comparable to their reported value of 6×10^{-3} s^{-1} and other values in literature ($1.3–4.0 \times 10^{-3}$ s^{-1}) [23,29]. The unusually high rate per mole Pt reported by Zhai et al. [8] for unpromoted Pt/Al_2O_3 allowed them to conclude that only a 10-times promotion was obtained upon addition of Na. Many factors can contribute to this apparent disagreement, starting from the nature of the Al_2O_3 support, the methods used for pretreating the catalysts after impregnation of precursors, and the difference in Na:Pt molar ratio.

To test the dependency on pretreatment, we report in Fig. 1 the rate per mole of Pt of $Pt/Na/Al_2O_3$ catalysts prepared by incipient wetness impregnation (IWI) and pretreated in two different ways as described in Section 2.1, that is, (1) calcination up to 250 °C, reduction up to 300 °C, passivation and exposure to air at RT, and (2) calcination up to 400 °C, only. For the same Na:Pt molar ratio of 20, we found that the first pretreatment resulted in a catalyst with 1.6 times higher rate per mole Pt than the one prepared by the second pretreatment. However, the same turnover frequency was obtained after normalizing the rate to the (lower) Pt surface measured by H_2 chemisorption (Table 1). The reduction in surface area was also observed on Pt/Al_2O_3–90Li prepared by calcination at 400 °C. For $Pt/Na/Al_2O_3$ samples prepared by calcination at 250 °C and reduction at 300 °C, the Pt dispersions estimated by EXAFS match well with the values from chemisorption (Table S3), suggesting that Pt was not covered by Na. A similar conclusion applies for the samples prepared by calcination at 400 °C because the dispersion values estimated by EXAFS were lower than or equal to the dispersion measured by chemisorption (Table S5). Thus, the data suggest that the higher calcination temperature induced Pt sintering. Note that in the case of $Pt/K/Al_2O_3$ catalysts, where the estimates of Pt dispersion by EXAFS are higher than those by chemisorption (Table S3), one cannot rule out the possibility of alkali migration on top of Pt particles.

The addition of alkali changed the WGS kinetics, particularly the water and CO_2 orders and the apparent activation energy. First, the increase in the water order on $Pt/Na/Al_2O_3$ catalysts (Table 1) can be the result of lower coverage of hydroxyl and hydroxyl-generating intermediates. This hypothesis was also supported by Panagiotopoulou and Kondarides [30] who proposed that the alkali increases the rate of decomposition of surface formates, which in turn consumes OH groups faster and lowers their coverage. The increase by 10–25 kJ mole^{-1} in E_a observed on Na-promoted catalysts can be explained by a change in adsorption energies of the reactant gases. Also, the change in CO, H_2O, H_2, and CO_2 orders suggests that Na modified the coverage of relevant surface species. The decrease in CO order suggests that alkali influenced the CO adsorption on Pt by strengthening the Pt—C bond, in agreement with claims in the literature [13–16]. Higher H_2O and H_2 orders are indicative of less exothermic (less negative) adsorption energies (ΔH_{H2O}, ΔH_{H2}). On the other hand, the negative CO_2 order reflects a more exothermic adsorption likely caused by the higher affinity of basic supports to re-adsorb CO_2 [31] and form carbonates [6,7,30].

From a more general point of view, we use the WGS kinetics as a basis for comparison between different catalysts. In that regard, the addition of Na to Pt/P25 and Pt/rutile had the same effect on the WGS kinetic parameters, as shown in Table 3. We observed changes in order in H_2O (from 0.68 to 0.8–1), H_2 (−0.6 to −0.3), and CO_2 (from 0 to ~−0.2), a decrease in CO order (by 0.2), and lower E_a. The similarities between $Pt/Na/Al_2O_3$ and $Pt/Na/TiO_2$ catalysts suggest that on both supports the same type of active site was created by the interaction with the alkali. The promotion of the rate, however, was less evident on TiO_2-supported catalysts than on $Pt/Na/Al_2O_3$. This is the direct outcome of the difference in TOF between the two alkali-free catalysts. Our results confirm that after the addition of Na, the TOFs of our best $Pt/Na/Al_2O_3$ (Pt/Al_2O_3–30Na) and Pt/P25–34Na are within a factor 2, as shown in Fig. 2. More importantly, the rates we measured on Pt/P25–34Na are consistent with recent findings by Zhu et al. [4] who reported a factor of 11 increase in TOF (300 °C) on a Pt/P25 after doping Na with the same alkali:Pt ratio of 34 (or 4 wt.%). Although we use the TOF at 300 °C to compare our results, we must point out that the increase in E_a we found on the Na-containing Pt/P25 catalyst was not evident in their study. The discrepancies in rate promotion and kinetics may be related to the exclusion of CO_2 in the feed stream in Zhu et al. [4], given that our data confirm that CO_2 inhibition occurs only on Pt–alkali samples. As can be noticed in Table 3, the alkali promotion shows a dependency on the structure of the TiO_2 (anatase vs rutile), possibly resulting from differences in the pore structure of each support that can influence how strongly the surface anchors Na species during catalyst preparation.

Although Li and K were also able to promote the rate of Pt/Al_2O_3, the change in WGS kinetics does not necessarily follow the same trend as for the catalysts promoted by Na. First, the maximum promotion effect of the TOF on $Pt/Li/Al_2O_3$ samples was obtained at an alkali:Pt molar ratio three times higher than on $Pt/Na/Al_2O_3$, and the maximum TOF was found to be three times lower compared to Pt/Al_2O_3–30Na (Table 1). Unlike for Na-promoted catalysts, the orders of reaction did not show sharp changes upon addition of Li. The water order progressively increased with Li

loading, reaching a maximum value of 0.83, and the CO_2 order was not as negative as seen for $Pt/Na/Al_2O_3$ samples. These parameters may indicate that Li was not influencing the relevant WGS steps as much as Na did or that (on average) Li is in lower proximity to Pt centers than Na. For example, Pt/Al_2O_3–12Li showed a TOF 10 times higher than Pt/Al_2O_3, whereas the increase was a factor of 17 on Pt/Al_2O_3–12Na. Another explanation for the lower H_2O order on Li-containing samples may come from the higher stability of LiOH ($\Delta H_f = -487$ kJ mole^{-1}) compared to that of NaOH ($\Delta H_f = -426$ kJ mole^{-1}). That is, the presence of less reactive OH groups on $Pt/Li/Al_2O_3$ compared to Na-promoted samples could result in smaller increase in water order. Following the same principle, the reactivity of OH groups (KOH, $\Delta H_f = -425$ kJ mole^{-1}) on K-promoted samples must be similar to that of $Pt/Na/Al_2O_3$ based on the increase in H_2O order. The increase in CO order with K addition, however, points to a different effect on the CO adsorption on Pt than was observed with Na or Li, and it exemplifies the dependency of E_a (~74 kJ mole^{-1}) on the CO order. The reason for lower surface coverage of CO on K-doped catalysts is unclear based on our data, but may be linked to the lower solubility of KNO_3 compared to the Na and Li precursors. When the aqueous alkali solutions contact the support, the solubility of the cations may influence their location with respect to Pt and the type of surface species formed during drying and affect subsequent activation and reaction. In spite of the different trend of the CO order, the rate on $Pt/K/Al_2O_3$ was promoted compared to the alkali-free catalyst, suggesting that the change in water order is more likely related to the rate enhancement. The rates normalized by surface Pt (TOF) were lower by a factor of 2 to that of $Pt/Na/Al_2O_3$ and about the same as the TOFs of the $Pt/Li/Al_2O_3$ series, when compared at the same alkali:Pt ratio. Overall, the observed promotion effect by alkali can be ordered as follows: Na > Li ~ K. This trend does not follow the Pauling or Sanderson electronegativities of the alkali oxides. Based on the kinetic data, the rate promotion must be the result of a combination of effects (i.e., water adsorption energy, alterations to CO adsorption and formation of carbonates) that maximizes the WGS rate with Na more than with other alkali species.

4.2. XAS during water–gas shift reaction

Selected alkali-promoted catalysts were analyzed by XAS in order to find correlations with the rate and the chemical state of Pt. Zhai et al. [8] explained the promotion effect of the WGS rates by proposing that alkali dopants increase the stability of oxidized Pt sites, which are suggested to be the true active sites. They support this claim based on Pt L_3 *in situ* XANES collected on $Pt/Na/SiO_2$ and $Pt/K/SiO_2$ (3:1 alkali:Pt molar ratio) which revealed the presence of cationic $Pt^{\delta+}$ on the fresh samples and after 1 h under WGS conditions (1% CO, 3% H_2O/He) at 275 °C. As shown in Fig. 3, our fresh (calcined 250 °C, reduced 300 °C, passivated and exposed to air) $Pt/Na/Al_2O_3$ catalysts also contained oxidized Pt, indicating that no reduction occurred due to the exposure of the catalysts to the X-ray beam. Other studies conducted in the same setup have also shown that Pt^{2+} and Pt^{4+} are observable and that the beam does not reduce Pt^{4+} [21]. We found that the intensity of the white line increased with the alkali content, suggesting that a greater percentage of Pt atoms are stabilized in the oxide state. Based on the estimation of particle size (Table S3), the decrease in the white line intensity on Pt/Al_2O_3–60Na can be explained by the presence of larger Pt particles (4–6.5 nm) which tend to remain more metallic. Changes in oxidation state were evidenced on all the $Pt/Na/Al_2O_3$ catalysts as they were analyzed under reducing H_2 mixture and WGS. Under both conditions, the *in situ* XANES for Pt/Al_2O_3–30Na (Fig. 4) demonstrates the complete reduction of Pt and the characteristic shift of the Pt edge and XANES due to CO adsorption. The XANES spectra in Fig. 5 show that (1) Pt was fully reduced under WGS conditions irrespective of the alkali loading and (2) CO adsorbed on metallic Pt since the shapes of the ΔXANES of $Pt/Na/Al_2O_3$ samples are similar to that of Pt/Al_2O_3. Note that the magnitude of the ΔXANES represents the amount of adsorbed CO normalized by the total amount of Pt. Therefore, the apparent trend observed in Fig. 5 results from the decrease in Pt dispersion with the addition of alkali and not from changes in CO coverage. The EXAFS fittings in Table S3 also revealed that $Pt/K/Al_2O_3$ exhibits fully reduced Pt under WGS conditions, with Pt particles much larger than for $Pt/Na/Al_2O_3$, in agreement with the dependency of pretreatment temperature and alkali content discussed in Section 4.1. The XAS data are in contradiction with the proposed model by Zhai et al. [8] that Pt oxides are the active sites for WGS. Our catalysts with Pt particle sizes in the 2–4 nm range exhibit comparable rates to those in [8], but showed no indication of Pt oxide formation under reaction conditions. Therefore, we propose that the alkali promotes metallic Pt sites by changing the properties of the surrounding material.

The XANES data shown in Table S4 support the claim that under certain circumstances the addition of alkali can stabilize Pt oxides. First, the data for Pt/Al_2O_3–20Na indicate that the method for catalyst preparation may be one of the contributing factors. When prepared by calcination at 250 °C followed by reduction at 300 °C, no PtO was detected on any of the $Pt/Na/Al_2O_3$ samples analyzed by XANES under WGS or after reduction *in situ* (Table S3). On the contrary, using calcination at higher temperatures changed the nature of the catalyst such that Pt partially remained in an oxidized state under reducing environments. As observed on both $Pt/Li/Al_2O_3$ and $Pt/Na/Al_2O_3$, the alkali:Pt ratio also influenced the fraction of PtO. That relative amount of oxidized Pt, however, did not track the rate promotion. While Pt/Al_2O_3–90Li showed a factor 1.4 higher rate per mole Pt than Pt/Al_2O_3–125Li, the former catalyst had a fraction of metallic Pt 1.7 times higher than that of Pt/Al_2O_3–125Li (Table S5). On Pt/Al_2O_3–20Na and Pt/Al_2O_3–90Na, the fraction of metallic Pt decreased by 1.6 times with alkali loading while the rate also decreased by a factor of 1.6. In other words, the rate per mole Pt increased with the fraction of metallic (not oxidized) Pt on the four samples that showed PtO. Since we were not successful in producing a catalyst with highly dispersed and stabilized oxidized Pt as the majority Pt species, we cannot rule out such a material as an alternate catalytic phase for WGS, but our results show clearly that Pt oxides are not the active sites for our catalysts, nor are such sites necessary to achieve TOFs in the range of 0.7 s^{-1} by promotion of Pt by alkali. Therefore, we propose that the active sites are metallic Pt clusters promoted by alkali oxides residing on the support.

5. Conclusions

Based on the kinetic evidence presented here, the addition of Na to Pt/Al_2O_3 and Pt/TiO_2 catalysts resulted in WGS rate promotion. On Pt/Al_2O_3, the alkali promoted the turnover frequency (250 °C, 6.8% CO, 8.5% CO_2, 21.9% H_2O, 37.4% H_2, and 1 atm.) by 107 times at our optimal 30:1 alkali:Pt molar ratio, whereas on Pt/TiO_2 the TOF at the same temperature and gas composition increased by four times (at a 34:1 alkali:Pt molar ratio). The rate per mole of surface Pt and the WGS kinetics were similar on $Pt/Na/Al_2O_3$ and Pt/Na/P25 catalysts, suggesting that the alkali modifies the support properties (not Pt) and creates new active sites. On both catalysts, an increase in H_2O and H_2 order was accompanied by lower CO and CO_2 orders and higher E_a. There is also promotion by Li and K on Pt/Al_2O_3. We found the promotion of the rate to follow the order Na > Li ~ K, with optimal alkali:Pt molar ratios between 30 and 50. The increase in water order in all cases can be interpreted as a decrease in surface coverage of water-generated intermediates

(hydroxyl, formates, and carboxylates) due to the influence of the alkali. The decrease in CO_2 order is likely to be related to the propensity of basic supports (alkaline) to form carbonates. These carbonates may compete for sites where the relevant support-generated intermediates can adsorb. The promotion of the rate by alkali must be a consequence of multiple effects on relevant steps in the reaction mechanism, possibly involving the adsorption energy for water and the perturbations to adsorbed species on the alkali support and Pt. XAS experiments revealed that the type of pretreatment used during catalyst preparation, and the type and loading of alkali can stabilize the formation of PtO. However, the *in situ* XAS evidence suggests that the promotion of the WGS rate by alkali is unrelated to the formation of Pt oxides. Platinum remains in metallic state, and we postulate that it serves as a conduit to adsorb CO in order for it to react with other intermediates from the support. Therefore, the promotional effect observed here can be categorized as a support effect.

Acknowledgments

The authors would like to thank Prof. Maria Flytzani-Stephanopoulos for instructive discussions and for sharing results with us. Support for this research was provided by the US Department of Energy, Office of Basic Energy Sciences, through the Catalysis Science Grant No. DE-FG02-03ER15466. Use of the Advanced Photon Source was supported by the US Department of Energy, Office of Basic Energy Sciences, under contract No. DE-AC02-06CH11357. MRCAT operations are supported by the Department of Energy and the MRCAT member institutions. Partial funding for JTM was supported by US Department of Energy, Office of Basic Energy Sciences, Division of Chemical Sciences, Geosciences and Biosciences. Argonne is operated by UChicago Argonne, LLC, for the US Department of Energy under contract DE-AC02-06CH11357.

Appendix A. Supplementary data

Supplementary data associated with this article can be found, in the online version, at doi:10.1016/j.jcat.2011.11.017.

References

[1] H.N. Evin, G. Jacobs, J. Ruiz-Martinez, U.M. Graham, A. Dozier, G. Thomas, B.H. Davis, Catal. Lett. 122 (2008) 9–19.
[2] H.N. Evin, G. Jacobs, J. Ruiz-Martinez, G.A. Thomas, B.H. Davis, Catal. Lett. 120 (2008) 166–178.
[3] P. Panagiotopoulou, D.I. Kondarides, J. Catal. 267 (2009) 57–66.
[4] X. Zhu, M. Shen, L.L. Lobban, R.G. Mallinson, J. Catal. 278 (2011) 123–132.
[5] X.L. Zhu, T. Hoang, L.L. Lobban, R.G. Mallinson, Catal. Lett. 129 (2009) 135–141.
[6] J.M. Pigos, C.J. Brooks, G. Jacobs, B.H. Davis, Appl. Catal., A 319 (2007) 47–57.
[7] J.M. Pigos, C.J. Brooks, G. Jacobs, B.H. Davis, Appl. Catal., A 328 (2007) 14–26.
[8] Y.P. Zhai, D. Pierre, R. Si, W.L. Deng, P. Ferrin, A.U. Nilekar, G.W. Peng, J.A. Herron, D.C. Bell, H. Saltsburg, M. Mavrikakis, M. Flytzani-Stephanopoulos, Science 329 (2010) 1633–1636.
[9] T. Shido, Y. Iwasawa, J. Catal. 141 (1993) 71–81.
[10] E. Chenu, G. Jacobs, A.C. Crawford, R.A. Keogh, P.M. Patterson, D.E. Sparks, B.H. Davis, Appl. Catal., B 59 (2005) 45–56.
[11] R. Burch, A. Goguet, F.d.r.C. Meunier, Appl. Catal., A 409–410 (2011) 3–12.
[12] C. Pedrero, T. Waku, E. Iglesia, J. Catal. 233 (2005) 242–255.
[13] J.C. Bertolini, P. Delichere, J. Massardier, Surf. Sci. 160 (1985) 531–541.
[14] E.L. Garfunkel, J.E. Crowell, G.A. Somorjai, J. Phys. Chem. 86 (1982) 310–313.
[15] J.E. Crowell, E.L. Garfunkel, G.A. Somorjai, Surf. Sci. 121 (1982) 303–320.
[16] N.D. Lang, S. Holloway, J.K. Norskov, Surf. Sci. 150 (1985) 24–38.
[17] G. Pirug, H.P. Bonzel, Surf. Sci. 199 (1988) 371–390.
[18] H. Tanaka, M. Kuriyama, Y. Ishida, S.I. Ito, K. Tomishige, K. Kunimori, Appl. Catal., A 343 (2008) 117–124.
[19] H. Tanaka, M. Kuriyama, Y. Ishida, S.I. Ito, T. Kubota, T. Miyao, S. Naito, K. Tomishige, K. Kunimori, Appl. Catal., A 343 (2008) 125–133.
[20] J.E. Benson, M. Boudart, J. Catal. 4 (1965) 704–710.
[21] J.H. Pazmiño, J.T. Miller, S.S. Mulla, W.N. Delgass, F.H. Ribeiro, J. Catal. 282 (2011) 13–24.
[22] J.T. Miller, A.J. Kropf, Y. Zha, J.R. Regalbuto, L. Delannoy, C. Louis, E. Bus, J.A. van Bokhoven, J. Catal. 240 (2006) 222–234.
[23] N. Guo, B.R. Fingland, W.D. Williams, V.F. Kispersky, J. Jelic, W.N. Delgass, F.H. Ribeiro, R.J. Meyer, J.T. Miller, Phys. Chem. Chem. Phys. 12 (2010) 5678–5693.
[24] L. Bollmann, J.L. Ratts, A.M. Joshi, W.D. Williams, J. Pazmino, Y.V. Joshi, J.T. Miller, A.J. Kropf, W.N. Delgass, F.H. Ribeiro, J. Catal. 257 (2008) 43–54.
[25] A. Hagemeyer, R.E. Carhart, K. Yaccato, A. Lesik, C.J. Brooks, C.B. Phillips, Platinum-alkali/alkaline-earth catalyst formulations for hydrogen generation, 2004.
[26] N.A. Koryabkina, A.A. Phatak, W.F. Ruettinger, R.J. Farrauto, F.H. Ribeiro, J. Catal. 217 (2003) 233–239.
[27] Y. Lei, J. Jelic, L.C. Nitsche, R.J. Meyer, J.T. Miller, Top. Catal. 54 (2011) 334–348.
[28] P. Panagiotopoulou, D.I. Kondarides, Catal. Today 127 (2007) 319–329.
[29] A.A. Phatak, N. Koryabkina, S. Rai, J.L. Ratts, W. Ruettinger, R.J. Farrauto, G.E. Blau, W.N. Delgass, F.H. Ribeiro, Catal. Today 123 (2007) 224–234.
[30] P. Panagiotopoulou, D.I. Kondarides, J. Catal. 260 (2008) 141–149.
[31] M.T. Xu, E. Iglesia, J. Phys. Chem. B 102 (1998) 961–966.